

# Dendrochronological analysis of coniferous trees in avalanche paths of Central Altai (Chuya River basin)

Nikolay I. Bykov<sup>1</sup>, Natalia V. Rygalova<sup>1</sup>, Anna A. Shigimaga<sup>1</sup>

**1** *Institute for Water and Environmental Problems, Siberian Branch of the Russian Academy of Sciences, 1, Molodeznaya St., 656038, Barnaul, Russian Federation*

Corresponding author: Nikolay I. Bykov ([nikolai\\_bykov@mail.ru](mailto:nikolai_bykov@mail.ru))

---

Academic editor: A. Matsyura | Received 22 October 2024 | Accepted 18 November 2024 | Published 5 December 2024

---

<http://zoobank.org/8C316B52-7FC4-40B7-8D1A-07704D078DE8>

---

**Citation:** Bykov NI, Rygalova NV, Shigimaga AA (2024) Dendrochronological analysis of coniferous trees in avalanche paths of Central Altai (Chuya River basin). *Acta Biologica Sibirica* 10: 1401–1418. <https://doi.org/10.5281/zenodo.14263406>

---

## Abstract

The performed dendrochronological analysis of the radial growth of coniferous trees in the avalanche paths of the Chuya River basin (Central Altai) has enabled to define the patterns of avalanche activity in the studied starting zones and the frequency of high-magnitude snow avalanches. It is shown that a tree-ring complex indicator is driving in detection of avalanche activity in specific avalanche paths. We suggest calling it the dendrochronological index of avalanche activity. In some cases, the applied dendrochronological method has helped to identify the cause (factor) of avalanching in the area under study.

## Keywords

Dendrochronological index of avalanche activity, Central Altai, Chuya, snow avalanches, tree rings, woody plants

## Introduction

Snow avalanches (SAs) are typical events in the mountainous areas where snow cover forms (Glaciological... 1984). Avalanching is triggered by a complex of reasons, including the constant factors of SA formation (altitude, steepness and exposure of slopes, their orientation relative to the main direction of air mass transfer),

as well as variable ones (snowfall intensity, duration and strength of wind, air and snow temperature, presence of loosened horizons and crusts in snow cover, etc.). This creates a variety of avalanche paths characterized by different avalanche activity (distance of avalanching, frequency of seasonal and long-term SAs) even within the same locality that complicates the observations of avalanche regime in specific avalanche paths. Despite the successful development of satellite monitoring of SAs, the information on avalanche activity is still insufficient. The matter is that such a monitoring covers two to three decades, whereas major avalanches, reaching low parts of tracks and accumulation zones, may occur with a frequency of several decades or even centuries. Therefore, to reconstruct the data on avalanche activity in specific avalanche paths, it is necessary to apply the indicative research methods.

Among such techniques, the dendrochronological method deserves prize for its reconstruction of dates and frequency of avalanches (Schweingruber 1993). With its help, the studies have been conducted worldwide: Kazakhstan (Zubairov et al. 2019), the Czech Republic (Tumajer, Tremel 2015), the USA (Martin, Germain 2016), Canada (Germain et al. 2016), Norway (Laute, Beylich 2018), Argentina (Mundo et al. 2007), Romania (Pop et al. 2017), Turkey (Köse et al. 2010), and other countries. The age of tree stands and vertical shoots of tilting trees, the values of heel coefficients (the ratio between the tree-ring width on heel and traction sides of a stem), the presence of compression wood, the cessation of tree growth (records of dead trees, their remains and mechanical damage), the presence of lightening effect (a sharp increase in growth owing to elimination of competing trees) (Kaennel, Schweingruber 1995), and the disruption of the anatomical structure of tree rings (traumatic resin ducts) are used as indicators of SAs (Perov et al. 1977; Kravtsova 1971; Turmanina 1979) (Fig. 1). Compression wood differs from the ordinary one by its abnormal structure and cells of high optical density. In coniferous trees, it is formed on a downslope side of stems (Kaennel and Schweingruber 1995). The heel side is the part of a tree stem facing downslope, and the traction part is the opposite side. Traumatic resin ducts (see Figure 1) emerge in wood as a result of stress in stems or insect-induced damage to crowns (Benkova and Schweingruber 2004).

As the mountain region, Altai is characterized by a significant diversity of both constant and variable factors of avalanche formation (Revyakin, Kravtsova 1977). In its inner regions (Central Altai), among major triggers of avalanching is the transformation of snow depth through its loosening. In frontal ridges, which block the air mass transfer, the crucial factor is snow accumulation. Since regular observations of SAs in Altai is absent, their long-term regime should be studied based on the indicative methods. Dendrochronological investigations of avalanches in Altai are small in number (Bykov, 2000) and mainly confined to Central Altai (Kravtsova 1971; Revyakin, Kravtsova 1976; Revyakin 1981; Surnakov 1985), including the Aktru Valley (Koroleva 1993; Nikolaeva, Savchuk 2021), and, to a lesser extent, to Northern (Kravtsova 1971), Northwestern (Revyakin, Kravtsova 1977; Bykov 2013; Bykov et al. 2024) and Northeastern Altai (Surnakov 1987). Some works present not only the dendrochronological data, but also the analyses of the influence of

avalanche processes on the composition and structure of plant communities that allows to estimate the rate of vegetation cover change in avalanche paths (Revyakin, Kravtsova 1977; Bykov 2013).

The work is aimed at analyzing the radial growth of coniferous species in the avalanche paths of the middle part of the Chuya River basin (Central Altai, right tributary of the Katun River) and dendrochronological reconstructing major avalanches in the studied avalanche paths (Fig. 2). In terms of avalanche activity, the study area located in Central Altai (Revyakin and Kravtsova 1977) is characterized by a certain combination of avalanche formation factors and significantly differs from the northwestern and northeastern parts of Altai. In this area, the dendrochronological studies and observations of SAs are rare (Revyakin and Kravtsova 1977; Bykov 2013; Nikolaeva and Savchuk 2021).

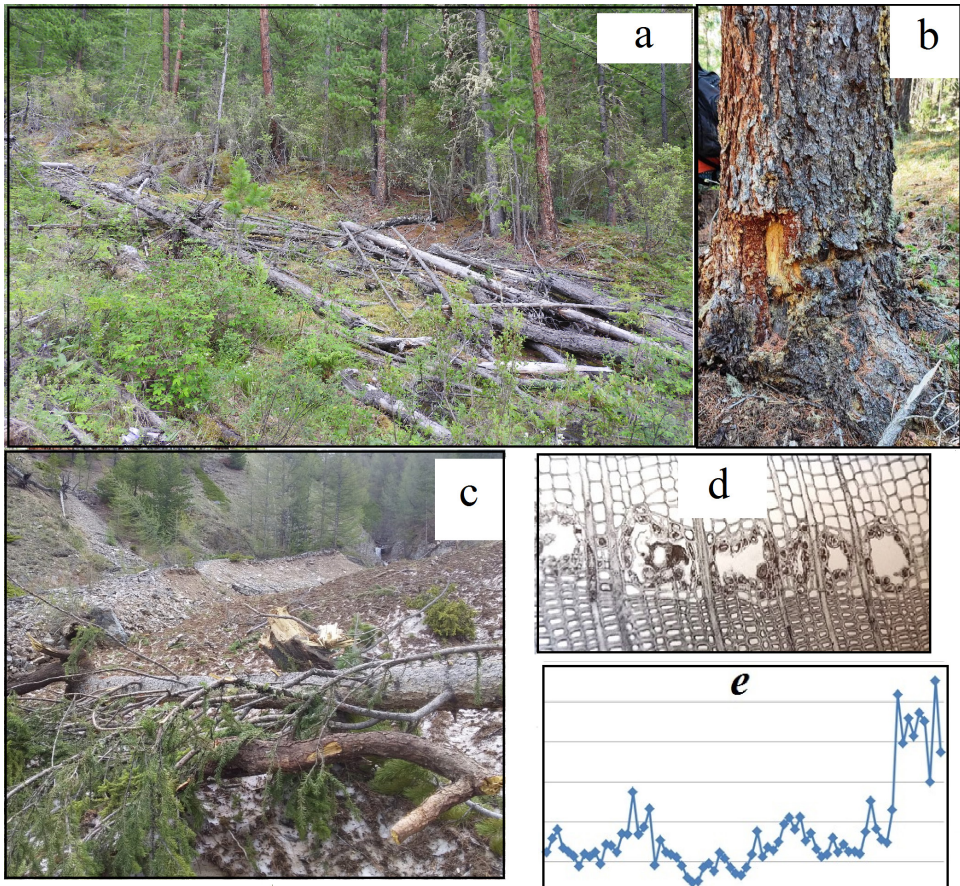


**Figure 1.** Signs of avalanche activity: **a** – tree death on the periphery of the accumulation zone in path 3 (photo 2022); **b** – wounds on tree stems caused by SAs; **c** – dead trees in the accumulation zone of path 1 (photo 2022); **d** – avalanche path 1; **e** – example of a sharp increase in radial increment in a tree (lightening effect).



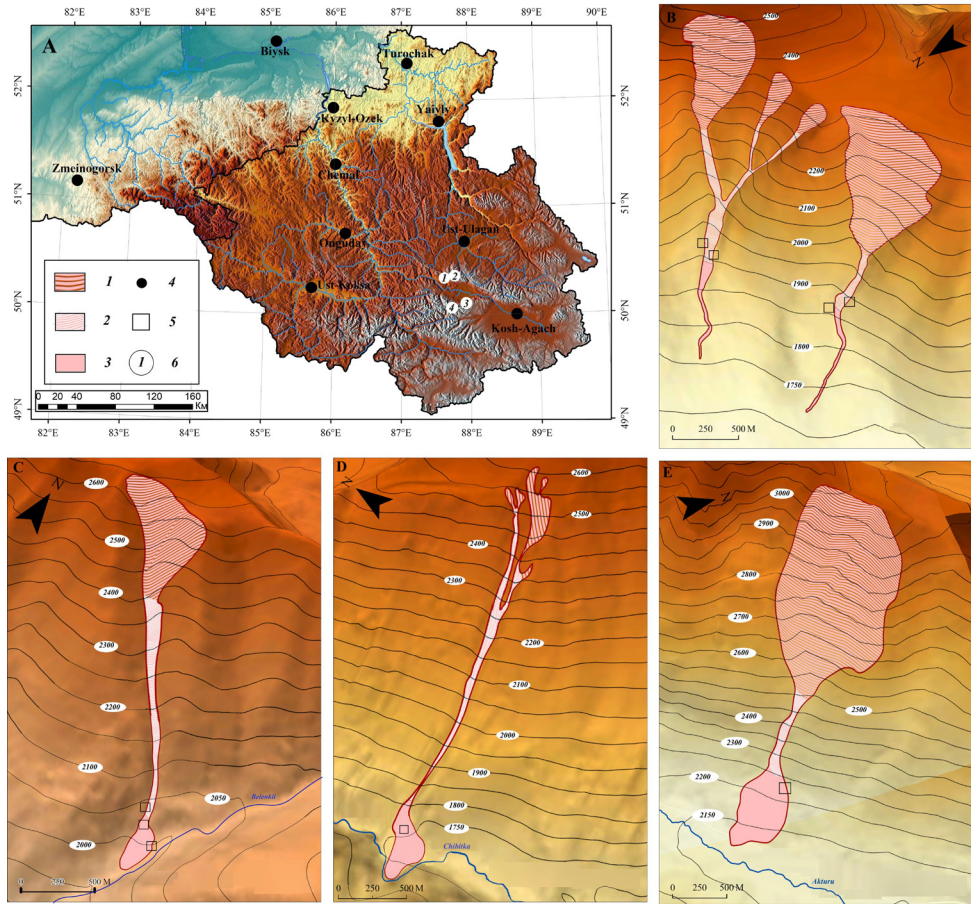


**Figure 2.** Sites of dendrochronological sampling in avalanche paths of the Chuya River basin (Central Altai). **A** – study area. Map legend: 1 – starting zone; 2 – track; 3 – accumulation zone; 4 – operating meteorological stations; 5 – sites of dendrochronological sampling; 6 – study areas. **B** – avalanche paths 3E (eastern) and 3W (western); **C** – avalanche path 2; **D** – avalanche path 1; **E** – avalanche path 4.

**Materials and methods**

Altai is distinguished by significant physical and geographical diversity related to avalanche processes. In Central Altai, avalanche activity is associated primarily with wind drifting accumulation, as well as heavy snowfalls and recrystallization of snow cover induced by sharp drops in air temperatures (Altai... 1978). Literature data (Revyakin, Kravtsova 1976) report about a 2-3-year rhythm of avalanche activity in the avalanche paths of this region. Here, SAs are powerful, avalanche paths are fully developed, forming mineral alluvial fans. Avalanche path density makes up 3-10 per 1 km of valley length (Altai... 1978). Numerous starting zones are located on slopes

with northern exposures thus indicating the influence both of snow accumulation with its maximum on leeward slopes (Galakhov 2003) and wind drifting on the development of avalanche processes.

In the Chuya River basin, we selected five avalanche paths (see Fig. 2): three on the North Chuisky Ridge, and two on the Kuraisky Ridge. In general, they are representative of the majority of avalanche paths in the Chuya River basin: starting zones with slopes of 28–38° (on average 32.0°) have northern and northwestern (with an azimuth of 323–357°), southwestern (251–258°) and southeastern (130–142°) exposures (Table 1). Avalanche trigger zones were discovered at altitudes of 2,325–3,065 m above sea level, and in low parts of the accumulation zone of avalanche snowfield - at altitudes 1,740–2,130 m (see Table 1).

**Table 1.** Characteristics of the studied avalanche paths

District number	Designation in Fig. 1	Avalanche paths	Starting zone	Coordinates of runout	Maximum altitude above sea level in the starting area, m	Number of starting zones	Minimum height above sea level of runout, m	Slope in the starting zone	Exposure, geographic azimuth
1	D		nord	50.3636	2660	2	1740	30.7	258
			sud	87.6334				37.6	251
2	C	-	-	50.3493 87.6868	2370	1	1985	27.9	142
3	B	east	east	50.1493	2510	3	1900	34.3	323
			center	88.0386				32.1	333
			west					30.0	357
	B	-	west	50.1464 88.0288	2325	1	1820	32.7	315
4	E	-	-	50.0817 87.7769	3065	1	2130	30.6	130

We established the location of avalanche snowfields in certain avalanche paths along their low edges (2013–2024) based on the analysis of spring images from Sentinel and Landsat satellites. The comparison analysis showed that avalanche activity here was not strictly synchronous (Fig. 3) because of differences in the geographic location of starting zones of SAs.

The object of our study was coniferous trees in the avalanche paths of the Chuya River basin (Table 2). Dendrochronological sampling was implemented in accumulation zones of these paths and low parts of tracks. This approach provides the reconstruction of major SAs having reached the accumulation zones or low parts of tracks. In addition, to get the local chronologies needed for the dendrochronologi-

cal reconstruction of dead trees, the samples of main tree species were previously collected outside the avalanche paths under study. Cores were extracted from living trees (i.e. the heel and traction sides of the stem at breast level), and in the starting zone – also at the tree base for individuals to determine their age. Tree cuts were sampled from dead trees with subsequent measurement of tree-ring widths along two radii. Species of dead trees were identified by means of anatomical analysis of wood (Benkova, Schweingruber 2004). As avalanche markers, the authors used the dates of tree death and damage, years of violation of synchronicity of increments on the traction and heel sides, the first year in a series of years of a abrupt change in the heel coefficient – the ratio of increment on the heel and traction sides of the stem, the presence of compression wood and traumatic resin ducts in xylem. Note that detection of traumatic resin ducts in tree rings is rather laborous). Chronologies were also studied for the presence of lightening effects, which in dendrochronology are interpreted as a sharp increment occurred due to tree stand thinning (Kaennel, Schweingruber 1995).

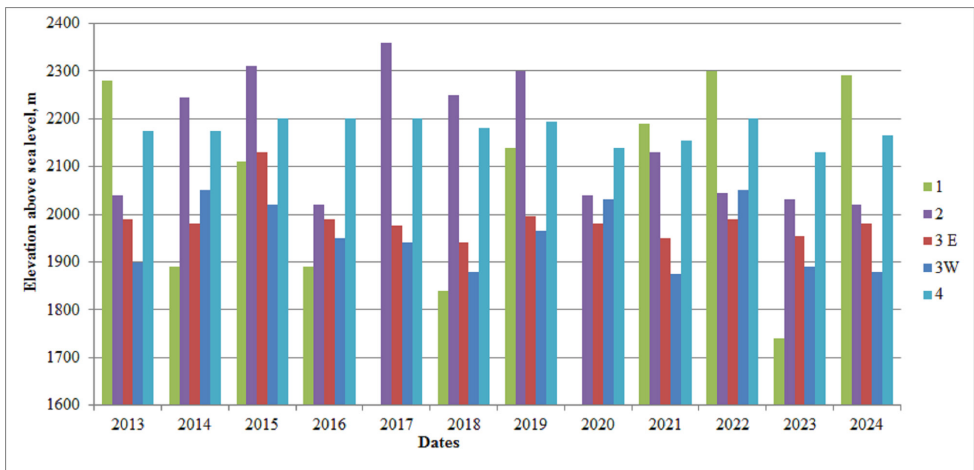


**Figure 3.** Location of the low edge of avalanche snowfields in the studied paths of the Chuya River basin in spring according to Sentinel and Landsat satellite data. Designations in the diagram: 1, 2, 3E, 3W, 4 – numbers of the studied avalanche paths (see Fig. 2).

Being non-specific, the above mentioned indicators of avalanche processes can be caused by various events. To improve SA indication, it is necessary to use the entire range of indicators. As an integral indicator of avalanching in a particular year, we used the ratio of the number of all cases of tree growth disturbances (specific indicators are given above) for this year to the number of studied trees. Previously, we proposed to call the ratio as the dendrochronological index of SA activity

$$x = \frac{a+b+c+d+e+f}{g},$$

where  $x$  is the dendrochronological index of avalanche activity for a certain year,  $a$  – the dates of tree death and injury,  $b$  – the violation of synchronicity of increment on the traction and heel sides,  $c$  – the first year in a series of the years characterized by an abrupt change in the heel coefficient,  $d$  – the presence of compression wood,  $e$  – the presence of traumatic resin ducts in xylem,  $f$  – the sharp increment (lightening effect),  $g$  – the number of trees examined. Tree-ring widths were measured using a semi-automatic Lintab 6 device with an accuracy of 0.01 mm. Standardization and generalization of the dendrochronological series were carried out in the ARSTAN program. In our case, Rbar (running correlation between series of tree-ring chronologies), EPS (the Expressed Population Signal) were used to assess the tree-ring chronologies of certain sites, while the mean sensitivity (Speer 2009) – in site chronologies. The latter were constructed if the EPS value was equal or higher than 0.85. For the reconstruction of the resulting chronologies, we employed the COFECHA program.

**Table 2.** Characteristics of the studied avalanche paths

Avalanche path number	Species	Sampling altitude above sea level, m	Number of trees examined	Calendar years of tree growth beginning	Calendar years of the last annual ring of trees	Age	Average correlation coefficient of chronologies from the traction and heel sides of a tree trunk	Rbar	EPS
1	<i>Larix sibirica</i> L.	1770–1800	19	1710–1997	2006–2022	35–315	0.57	0.18	0.81
	<i>Picea obovata</i> L.		4	1796–1965	1986–2022	48–225	0.77	0.38	0.71
	<i>Pinus sibirica</i> Du Tour		8	1919–1983	1981–2022	17–103	0.62	0.13	0.54
2	<i>Pinus sibirica</i> Du Tour	1980–2010	18	1777–1903	1995–2023	40–155	0.70	0.49	0.94
	<i>Picea obovata</i> L.		2	1929, 1951	2003, 2023	72, 74	0.80	0.54	0.70
	<i>Larix sibirica</i> L.		9	1842–2001	1998–2023	17–126	0.82	0.46	0.88
3W	<i>Larix sibirica</i> L.	1850–1870	39	1777–2001	1927–2024	21–215	0.90	0.55	0.98
	<i>Picea obovata</i> L.		4	1877, 1945	2022–2024	81–169	0.59	0.70	0.90
	<i>Pinus sibirica</i> Du Tour		10	1843–1905	1992–2022	47–152	0.72	0.62	0.94
3E	<i>Larix sibirica</i> L.	1895–1990	17	1612–1999	2013–2022	23–409	0.63	0.19	0.80
	<i>Picea obovata</i> L.		6	1872–1920	1982–2023	102–150	0.59	0.25	0.67
	<i>Pinus sibirica</i> Du Tour		7	1511–1969	1922	53–511	0.72	0.35	0.79

Avalanche path number	Species	Sampling altitude above sea level, m	Number of trees examined	Calendar years of tree growth beginning	Calendar years of the last annual ring of trees	Age	Average correlation coefficient of chronologies from the traction and heel sides of a tree trunk	Rbar	EPS
4	<i>Larix sibirica</i> L.		1	1924	2022	98	0.79	-	-
	<i>Pinus sibirica</i> Du Tour	2130–2140	3	1528–1935	2022	87–494	0.59	0.16	0.36

Note: Dash indicates not calculated values, Rbar is the average interserial correlation coefficient, EPS is the population signal.

## Results and discussion

Age analysis of living and dead trees in the studied avalanche paths suggests that age naturally increases in the track from the trough to the stand beyond the avalanche path. The onset of trees' growth in the low part of the track in path 1 dates back to 1707–1997 (for *Picea obovata* L. – 1796–1965, *Pinus sibirica* Du Tour – 1919–1983, *Larix sibirica* L. – 1710–1997) (Table 2). The age of the trees studied in path 1 ranged from 17 to 315 years, averaging to 105 years. Of dead trees, only two were examined – *Pinus sibirica* Du Tour aged 76 and *Larix sibirica* L. aged 134 years. In path 2, the beginning of stand growth along the periphery of the accumulation zone dates back to 1868–2007 (for *Picea obovata* L. - 1929 and 1951, *Pinus sibirica* Du Tour 1777–1903, *Larix sibirica* L. - 1842–2001); in avalanche path 3W – to 1708–2001 (for *Picea obovata* L. - 1877 and 1945, *Pinus sibirica* Du Tour 1843–1905, *Larix sibirica* L. - 1777–2001); in path 3 E - to 1511–1999 (for *Picea obovata* L. – 1872–1920, *Pinus sibirica* Du Tour 1511–1969, *Larix sibirica* L. – 1612–1999); in path 4 – to 1528–1935 (for *Pinus sibirica* Du Tour - 1528–1935, *Larix sibirica* L. - 1924). The age of the trees studied in path 2 varied from 14 to 155 years (on average 84 years), in 3W – from 17 to 287 (on average, 129 years), in 3E – from 6 to 511 (on average, 143 years), and in path 4 – from 87 to 494 years (on average, 278 years). In avalanche paths 2 and 3, we examined dead trees (two *Larix sibirica* L. aged 58 and 120 years and one *Pinus sibirica* Du Tour aged 103 years); in 3W – 10 (2 *Pinus sibirica* Du Tour aged 81 and 138, 8 *Larix sibirica* L. aged from 29 to 283 years); in 3 E – 7 (2 *Pinus sibirica* Du Tour aged 140 and 144 years, 3 *Larix sibirica* L. – 41, 261 and 409 years, 2 *Picea obovata* L. – 102 and 113 years). In avalanche path 4, 4 trees were felled by SAs in the year of sampling (3 *Pinus sibirica* Du Tour and 1 *Larix sibirica* L., their age is given above). Age of living and dead trees indicates that avalanching occurs with different frequencies. The time interval between the most powerful avalanches is 490–510 years. The interval between less powerful events can reach 260–285 years. The frequency of medium-magnitude avalanches is 40–145 years. Major SAs,



which destroyed 490–510 year trees, were recorded in 2011 and 2022. Trees aged 260–285 years perished in 1995 and 2019, and 40–145-year olds – during the period 1954–2023. As a rule, the dates of the last ring of a dead tree and SA occurrence differ by one year. However, in some cases they may coincide. This is due to the fact that sometimes damage to tree stems happens in places above low branches. During the subsequent vegetation period such trees have time to form several rows of xylem cells. Hence, when making records of dead trees, anatomical analysis of the last tree ring is a must. In general, the age analysis of living and dead trees is evidenced of increased intensity of SAs in the last 20 years. One possible reason for this is the increase in winter precipitation during this period.

Mechanical damage (wounds) to trees in avalanche paths of the study area of Central Altai significantly differs from that in Northwestern Altai. In the latter, tree wounds appear as a result of hits by broken tree stems brought with SAs. In Central Altai, avalanches mostly consist of rocky debris, being indicative feature and most common in the Chuya River basin. Reconstruction of mechanical damages to trees clearly demonstrates the increase in their number in the last 20 years along with the general trend of growing winter precipitation in the study area (Fig. 4). High precipitations were recorded in 2009–2011 and 2017–2023. Comparison of the number of damages with the precipitation amount for October–March according to the Kosh-Agach and Ust-Ulagan weather stations shows that SAs are not always caused by the increased snow reserves at the end of winter. For example, they occurred in avalanche path 3 W in 1998 despite small snow reserves in snow cover. Similar situation was noted in 1982 in avalanche path 1. In the year 2010, characterized by high winter precipitations, January avalanches occurred in conditions of anticyclonic weather with frosts up to  $-30$  –  $-40^{\circ}\text{C}$ ; SAs were triggered by snow thickness transformation. Thus, the presence of wounds does not allow us to accurately determine SAs factors. It should be borne in mind that the presence of a large number of tree damages in the last 20 years can be explained by healing undetected wounds appeared in the previous years.

An abrupt increase in increment (lightening effect) in individual chronologies obtained from the trees of avalanche paths is also rarely detected. Along the edge of avalanche path 1, such an effect was manifested in 1978 only in two spruces – 1st (aged 136 years) in 1961, and 2nd (aged 145 years). In avalanche path 3 W, it was noted in two larches – 1st (aged 157 years) in 2014, and 2nd (aged 10 years) in 2011. Compression wood was found in rings of seven trees in path 1, 4 trees in path 2, 6 trees in 3W, 7 trees in 3E. In avalanche path 1, reactive wood was detected in 3d (1969), 4th (1970) and 35th year (2001) of life of the first tree (larch). Compression wood was identified in the rings of 2nd tree (larch) in 1960, 1961, 1964 and 1966 (at the age of 3, 4, 7 and 9 years, respectively); 3d tree (larch) at the age of 36–39 – in 2009–2012; 4th tree (spruce) – at the age of 166–169 years (1978–1981), 5th (spruce) – at the age of 105 (1938), sixth (spruce) – at the age of 43 (1863); 7th tree (cedar) – at the age of 36 (2013), 37 (2014) and 41 (2018) years. No synchronicity in manifestation of tree rings with reactive wood was found in trees of this avalanche path.

In avalanche path 2, tree rings with compression wood were found in two larches aged 5 and 6 (1910, 1911) and 10–13 (2013–2016), including two cedars aged 33 (1997) and 122–124 (1996–1998) years. In path 3W, compression wood was detected in trees aged 7–9 (1855–1857), 10 (1877), 10–14 (2011–2015), 29–31 (1899–1901), 85 (2000), and 100 (1876). In path 3E, tree rings with such wood were revealed in trees aged of 8–10 (1912, 1913, 1977–1979), 12–16 (2011–2015), 24 and 25 (2010, 2011), 25–27 (1926–1928), 40–43 (1961–1964), 53–55 (1953–1955), 94–107 (1995–2008), 273 (1885) years. Thus, synchronicity in manifestation of compression wood in trees of other avalanche paths is also rare. Most often, compression wood is formed in trees at an early age highly likely because of snow pressure on plants.

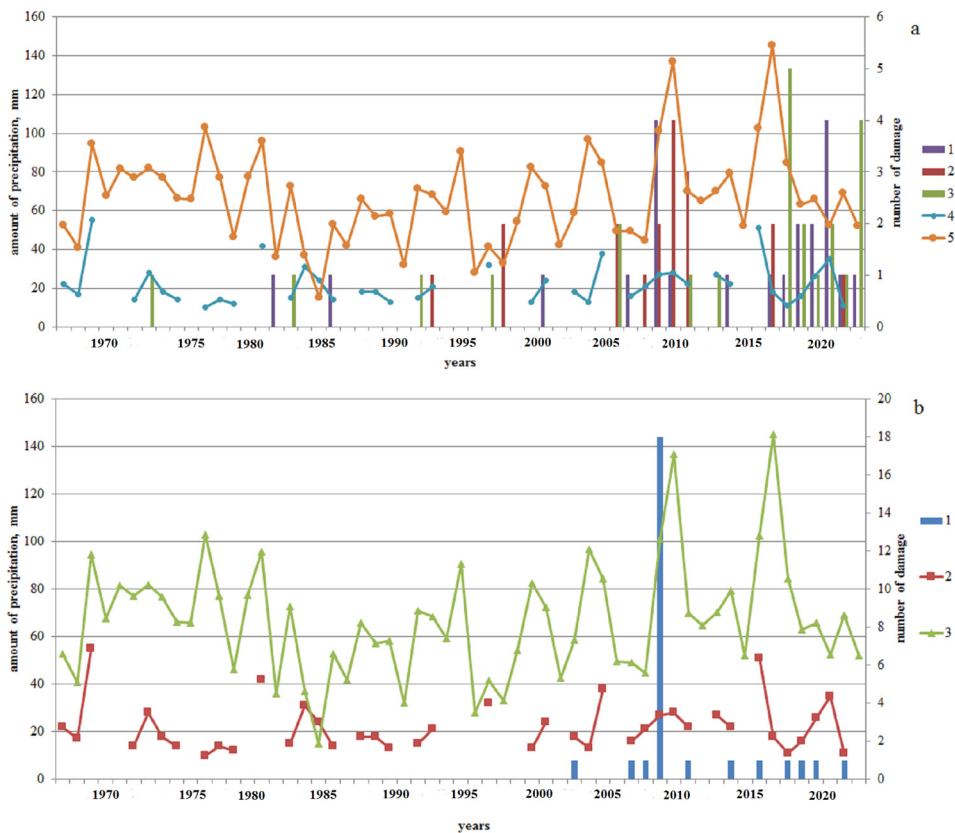


**Figure 4.** The ratio of the number of cases of mechanical damage to trees in avalanche paths of the Chuya River basin and total precipitation. Designations in the diagram (a): 1 – avalanche path 1; 2 – avalanche path 4; 3 – avalanche path 3W; 4 – precipitation for October–April according to the Kosh-Agach meteorological station; 5 – precipitation for October–April according to the Ust-Ulgan meteorological station; b) 1 – avalanche path 2; 2 – precipitation for October–April according to the Kosh-Agach meteorological station; 3 – precipitation for October–April according to the Ust-Ulgan meteorological station.

Traumatic resin ducts in rings of trees from avalanche paths are present much more often, as compared to compression wood. They are found on the heel and the traction sides of tree stems. Synchronicity in their distribution is weak in different avalanche paths, in trees from the same path, and even on different sides of the stem. At best, such ducts are concurrently detected only in a quarter of the trees studied in the avalanche path. The frequency of occurrence of traumatic resin ducts depends less on tree age than compression wood occurrence. In avalanche path 1, traumatic resin ducts were found in the entire sample of the studied trees for 1722, 1732, 1736, 1738, 1742, 1744, 1747, 1749, 1752, 1753, 1762, 1765, 1767, 1768, 1774, 1776, 1780, 1793, 1798, 1800, 1806, 1817, 1828, 1841, 1844, 1846, 1853–1855, 1858, 1860, 1864, 1867–1869, 1875, 1877, 1878, 1882, 1883, 1885, 1891, 1892, 1894, 1902, 1908, 1909, 1918, 1919, 1926, 1928, 1934, 1936, 1938, 1940, 1941, 1943, 1944, 46, 1948, 1950, 1953, 1955, 1957, 1966–1972, 1974, 1977, 1979, 1981–1984, 1986–1992, 1994–2014, 2016–2018, 2020, 2022. Hence, traumatic resin ducts were noted approximately in every fifth year during the 1707–2022 period.

In avalanche path 2, this indicative sign was present much less frequently: 1934, 1948, 1968, 1969, 1997, 1998, 2002, 2010, 2016, 2018. In 3W, it was recorded for the years 1846, 1850, 1855, 1862, 1964, 1866, 1867, 1870, 1871, 1873, 1882–1884, 1887, 1890–1894, 1896, 1898, 1902–1909, 1915, 1917, 1925, 1927, 1929, 1932, 1937, 1938, 1948, 1950, 1955, 1957, 1960–1963, 1967, 1969–1971, 1976–1978, 1981, 1984, 1987, 1989, 1992, 1994, 1996–1998, 2010, 2015–2018, 2021. There was no synchronicity in distribution of traumatic resin ducts either. Maximum number of trees (4 out of 30 examined) with such ducts was concurrently recorded in 2010. In avalanche path 3E, traumatic resin ducts were found in tree rings in 1810, 1818, 1948, 1853, 1857, 1866, 1879, 1882, 1884–1886, 1892, 1894–1897, 1899, 1900, 1908–1910, 1917, 1919, 1921, 1923, 1938–1942, 1944, 1948, 1959, 1963, 1966, 1969, 1972, 1975–1977, 1987, 1988, 1993, 2006, 2007, 2009–2019, 2022. Here, not more than 15% of the examined trees in this path simultaneously contained such ducts.

Signs of SA impacts on trees can be detected from asynchronous increment on different sides of stems that is usually noted in the year of SA occurrence. Typically, in the vegetation season of a given calendar year, an increment on one side of the stem increases, while on the other decreases. An increase in increment on one side can last for several years until the stem takes a vertical position. As a tree ages, the period of restoration of its stem verticality takes more time. Therefore, the year of SA event can be most accurately defined from the first year of asynchronous increment. This makes it difficult to reconstruct avalanches in subsequent years. Important, uneven growth can also be caused by other reasons, e.g. snow creep from a slope or wind exposure. Concurrent asynchrony in increment is observed on average in 15–20% of trees, but in some years it can be higher. If the number of trees examined in an avalanche path is 10 or more, then asynchrony is detected in about half of them. For instance, in 1856, it was observed in 53% of trees from path 3W; in 1828 – in 63% of trees from 3E; in 1922 – in 50% of trees from path 2, and in 64% of trees from avalanche path 1. However, if the number of studied trees is insignificant (1–4), asynchrony can reach 75–100% in a given year.

One of the dendrochronological indicators of uneven radial growth and, accordingly, SA indicator is the heel coefficient (Kravtsova 1971; Revyakin, Kravtsova 1976), which is the ratio of the stem increment on the heel side to that on the traction side in coniferous tree species. This difference occurs because traction wood is weaker than heel wood in conifers. In the year of avalanching, this coefficient greatly increases. However, it also characterizes the presence of inertia. For instance, after the first year of its rapid growth, a further smooth increase can be observed for several years, without SA impacts. In this case, the heel coefficient may grow both with synchronous and asynchronous increment on the opposite sides of the stem. Some researchers use the heel coefficient to determine SAs magnitude (Kravtsova 1971). However, in our opinion, the value of this coefficient is an unreliable criterion for determining the power of an avalanche. A more suitable method for establishing the power of avalanches is the choice of the location for collecting dendrochronological samples, since the power of avalanches and the distance of their ejection are usually interrelated.

The analysis suggests that synchronicity of increment occurrence on the heel and traction sides of tree stems in the studied paths is often violated: once every 2-7 (on average 3.7 years). At the same time, a strong similarity between them exists despite synchronicity violation (Table 2). The average (for tree species) correlation coefficients of chronologies for heel and traction sides vary within 0.57 - 0.90. In the track, the similarity is higher for stands along the edge of the avalanche path than for trees growing closer to the avalanche chute. Paired correlations of chronologies for the heel and traction sides in the accumulation zone are lower than along the edge of the avalanche path or beyond it. A similar situation is revealed for the inter-serial correlation coefficients of chronologies: they are greater along the path edge than in the track. Also, the population signal (EPS) of trees outside the avalanche path is higher than that within it. All this supports the fact that trees in the path experience SA impacts already at the stage of their growth. Among tree species, *Picea obovata* L most often demonstrates the worst indicators of EPS.

Some researchers state that a complex dendrochronological analysis is a must for indicating snow avalanches (Germain et al. 2010). In our study, the ratio of the sum of all cases of growth disturbances (increment asynchrony, a sharp increase in the heel coefficient, the presence of compression wood and traumatic resin ducts, the lightening effect, the dates of death and wound formation) in trees studied in the low part of the track and accumulation zone to their number served as an indicator of SAs. We proposed to call this ratio the dendrochronological index of avalanche activity (Bykov et al. 2024).

The obtained dendrochronological data on SAs were confirmed by remote sensing data (2013–2024) from Sentinel and Landsat satellites (see Fig. 3), as well as by the results of ground observations. During this period, major SAs in avalanche path 1 were observed in 2016, 2018; values of the dendrochronological avalanche activity index made up 0.7 and 0.6. In path 4, this index (2020, 2023) was equal to 1.3 and 1.0, respectively. In other studied paths, avalanches did not reach the sites

of dendrochronological sampling during this period. If an index value of 0.6 and above is assumed as a criterion for occurrence of high-magnitude SAs in other time periods, then in path 1 during the 1707–2022 period avalanche events could happen in 1722, 1726, 1732, 1738, 1744, 1747, 1752, 1753, 1756, 1760, 1762, 1764, 1766, 1767–1769, 1774, 1780, 1785, 1787, 1791, 1794, 1798, 1799, 1805, 1806, 1808, 1811, 1814, 1816, 1817, 1821, 1823, 1828, 1830, 1841, 1843, 1845–1847, 1851, 1853, 1855, 1856, 1860, 1861, 1863, 1864, 1866, 1868, 1869, 1871–1873, 1875, 1877, 1878, 1883, 1885, 1891, 1895, 1905, 1906, 1908–1910, 1914, 1915, 1917, 1919, 1920, 1922, 1927, 1930, 1932, 1935, 1938, 1943, 1946, 1947, 1948, 1955, 1961, 1965, 1974, 1980, 1985, 1987, 1992, 1996, 2001, 2004, 2007, 2009, 2010, 2016, 2018 (Table 3). Thus, major SAs in this avalanche path occurred approximately once every three years over 295 years. In the 20th century, such avalanches occurred 36 times, as follows from the dendrochronological studies.

In path 2, high-magnitude SAs were recorded much less frequently: in 1886, 1890, 1902, 1903, 1909, 1914, 1922, 1923, 1930, 1961, 1966, 1996, 2001, 2010 (once every 10 years on average). In the last century, major SAs were observed 12 times.

In avalanche path 3E, over more than the 500-year period (1511–2022), major avalanche events occurred in 49 years; approximately, once every 10 years (Table 3), including 9 times in the 20th century.

**Table 3.** Years of major SAs in the studied paths of the Chuya River basin (Central Altai)

Avalanche path number	Years of maximum avalanches
1	1722, 1726, 1732, 1738, 1744, 1747, 1752, 1753, 1756, 1760, 1762, 1764, 1766, 1767–1769, 1774, 1780, 1785, 1787, 1791, 1794, 1798, 1799, 1805, 1806, 1808, 1811, 1814, 1816, 1817, 1821, 1823, 1828, 1830, 1841, 1843, 1845–1847, 1851, 1853, 1855, 1856, 1860, 1861, 1863, 1864, 1866, 1868, 1869, 1871–1873, 1875, 1877, 1878, 1883, 1885, 1891, 1895, 1905, 1906, 1908–1910, 1914, 1915, 1917, 1919, 1920, 1922, 1927, 1930, 1932, 1935, 1938, 1943, 1946, 1947, 1948, 1955, 1961, 1965, 1974, 1980, 1985, 1987, 1992, 1996, 2001, 2004, 2007, 2009, 2010, 2016, 2018
2	1886, 1890, 1902, 1903, 1909, 1914, 1922, 1923, 1930, 1961, 1966, 1996, 2001, 2010
3E	1513, 1515, 1518, 1521, 1524, 1531, 1537, 1539, 1543, 1552, 1558, 1563, 1569, 1586, 1589, 1601, 1603, 1610, 1625, 1648, 1651, 1665, 1670, 1681, 1684, 1687, 1693, 1707, 1714, 1719, 1721, 1750, 1797, 1803, 1811, 1828, 1846, 1860, 1892, 1894, 1926, 1927, 1932, 1939, 1947, 1954, 1961, 1973, 1987
3W	1856, 1859, 1871, 1898, 1915, 1916, 1936, 1937, 1953, 1989, 1993, 1994, 2006, 2010, 2011
4	1529, 1531, 1533, 1535, 1539, 1540, 1544, 1550, 1552, 1558, 1560, 1564, 1568, 1574, 1578, 1580, 1581, 1584, 1597, 1600, 1605, 1607, 1615, 1620, 1624, 1631, 1632, 1647, 1650, 1652, 1659, 1663, 1666, 1670, 1672, 1676, 1681, 1685, 1693, 1695, 1699, 1700, 1704, 1706, 1717, 1725, 1726, 1734, 1736, 1746, 1748, 1756, 1758, 1759, 1763, 1765, 1769, 1771, 1772, 1773, 1774, 1777, 1779, 1781, 1792, 1799, 1805, 1809, 1817, 1823, 1828, 1832–1834, 1839, 1844, 1845, 1857, 1859, 1861, 1866, 1869, 1871, 1879, 1883, 1886, 1889, 1892, 1895, 1896, 1901, 1902, 1906, 1911, 1914, 1919, 1922, 1926, 1929, 1936, 1939, 1940, 1955, 1959, 1961, 1973, 1975, 1976, 1977, 1979, 1985, 1999, 2002, 2004, 2017, 2019, 2020, 2023



In path 3W, they were recorded in 1856, 1859, 1871, 1898, 1915, 1916, 1936, 1937, 1953, 1989, 1993, 1994, 2006, 2010, 2011 (once every 16 years on average). In last century, they were noted 11 times.

Finally, high-magnitude snow avalanches occurred in path 4 in 1529, 1531, 1533, 1535, 1539, 1540, 1544, 1550, 1552, 1558, 1560, 1564, 1568, 1574, 1578, 1580, 1581, 1584, 1597, 1600, 1605, 1607, 1615, 1620, 1624, 1631, 1632, 1647, 1650, 1652, 1659, 1663, 1666, 1670, 1672, 1676, 1681, 1685, 1693, 1695, 1699, 1700, 1704, 1706, 1717, 1725, 1726, 1734, 1736, 1746, 1748, 1756, 1758, 1759, 1763, 1765, 1769, 71, 1772, 1773, 1774, 1777, 1779, 1781, 1792, 1799, 1805, 1809, 1817, 1823, 1828, 1832–1834, 1839, 1844, 1845, 1857, 1861, 1866, 1869, 1871, 1879, 1883, 1886, 1889, 1892, 1895, 1896, 1901, 1902, 1906, 1911, 1914, 1919, 1922, 1926, 1929, 1936, 1939, 1940, 1955, 1959, 1961, 1973, 1975, 1976, 1977, 1979, 1985, 1999, 2002, 2004, 2017, 2019, 2020, 2023 (on average, once every 4 years). In the 20th century, avalanching was observed 28 times.

The distribution of major SAs in specific avalanche paths by centuries has minor differences. SAs number is greatly influenced by constant factors of avalanche formation: exposure, slope gradient, altitude of starting zones. Avalanche paths 1 and 4 turned out to be most active. They differed from others, first of all, by high location of fracture line in starting zones. This factor is also responsible for intensity of major SAs in path 3E, as compared to 3W. The latter two are situated next to each other and have similar constant factors of avalanche formation.

Synchronicity of major SAs in different paths is low (Table 4). In terms of equal time intervals, the greatest synchronicity was demonstrated by paths 1 and 4, as well as 1 and 2 (Table) where powerful avalanching occurred 8 times in the same year during the 20th century. If the first pair of avalanche paths are similar in the altitude position of starting zones, then the second is characterized by their geographical proximity. In the pair –1 and 3E – high-magnitude avalanche events appeared in the same year 5 times during the 20th century. In 1961, such avalanches were recorded in four out of five studied paths, and in 1922, 2010 – in three paths. In the winter season of 2009–2010, SAs were caused by high (October–March) precipitations. However, since in the winter of 1960–1961 this region saw the mean precipitation amount, probably, another climatic factor was crucial. Clearly, it needs additional studies of meteorological factors for this year. In 1996, avalanches were noted in paths 1 and 2. Here, the winter of 1995–1996 was characterized by an extremely low amount of atmospheric precipitation and avalanching was obviously induced by recrystallization of snow depth. Similar conclusions about the causes of avalanches in this region have been made by other researchers (Altai... 1978; Revyakin 1981). From this follows the methodological conclusion that establishing the causes of avalanches using the tree-ring indication method outside the period of instrumental meteorological observations in this region is hardly possible.

In contrast to the Korgon River basin (Northwestern Altai), an attempt to derive the dendrochronological index of avalanche activity for the Chuya River basin was unsuccessful (Fig. 5), (Bykov et al. 2024). Generalization of this index for the basin

leads to its averaging and underestimation (only twice over the past 500 years its value reached 0.6). This can be explained by significant difference in constant factors of SA formation in the avalanche paths that results in asynchronous avalanching.

It should be also borne in mind that the value of the dendrochronological index of avalanche activity is affected by the number of trees studied in the paths. For example, if one tree is studied in the avalanche path, the index value as an indicator of avalanching must be equal or above 1.0. However, with a rising number of studied trees, the index of SA indication decreases. This confirms the conclusions of other researchers about the minimum number of trees studied when conducting tree-ring indication (Germain et al. 2010). The results about the descent of maximum avalanches with a smaller number of trees studied should be perceived as evaluative. They can probably be confirmed or refuted by additional selection of dendrochronological samples at higher levels in the transit zone.

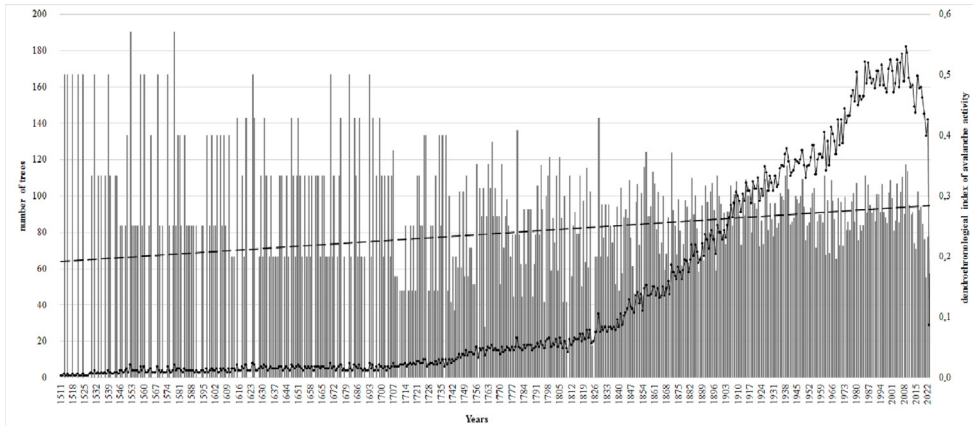


**Figure 5.** Changes in the dendrochronological index of avalanche activity generalized for the Chuya River basin according to the dendrochronological data (columns) and the number of trees studied (line). The dotted line indicates the trend in the dendrochronological index of avalanche activity.

**Table 4.** Years of synchronous SAs in the studied avalanche paths

Avalanche path number	1	2	3E	3W
2	1909, 1914, 1922, 1930, 1961, 1996, 2001, 2010	-	-	-
3E	1927, 1932, 1947, 1961, 1987	1961	-	-
3W	1915, 2010	2010	-	-
4	1906, 1914, 1919, 1922, 1955, 1961, 1985, 2004	1902, 1914, 1922, 1961	1926, 1939, 1961, 1973	1936

## Conclusions

The ratio of dendrochronological indicators of SAs largely differs for Central and Northwestern Altai. In Central Altai, with the growing role of mechanical damage to tree stems, the importance of traumatic resin ducts declines because of cumbersome determination of the latter. Since all avalanche indicators are non-specific (they can be caused by other factors), it is necessary to use a set of indicators to reduce reconstruction errors. The dendrochronological index of avalanche activity, which is the ratio of the number of cases of tree growth disturbance to the number of trees studied, can serve as an indicator of SAs. However, its generalization for the studied basin is impractical due to significant diversity of constant factors of avalanche formation (exposure and gradient of slopes, altitude of starting zones (a.s.l), etc.).

Based on the performed dendrochronological analysis, we have revealed a weak synchronicity of major SAs in the studied paths. It increases with closer proximity of avalanche paths and higher similarity of their constant factors of avalanche formation (primarily, altitude of starting zones).

Using the dendrochronological method, we have established that various factors (intensive snow accumulation in winter (2010), recrystallization of snow thickness (1996)) are responsible for major SAs in the Chuya River basin. To identify the factors of major SA in certain years, for example in 1961, an additional analysis of meteorological indicators is needed. The trend towards increasing winter precipitation in the study region will likely result in the formation of more intensive SAs and increased risks to human life.

## Acknowledgement

The study was supported by the grant of the Russian Science Foundation No. 24-27-00123 “Response of avalanches in the inland mountainous area to climate change”, <https://rscf.ru/project/24-27-00123/>.

## References

- Altai Territory (1978) Atlas (in 2 volumes). T. 1. Moscow, Barnaul, 222 pp. [In Russian]
- Benkova VE, Schweingruber FKh (2004) Anatomy of wood plants in Russia. Publishing House «Haupt», Bern, 465 pp.
- Bykov NI (2000) Dendrochronology of snow avalanches and atmospheric circulation processes in the winter and transitional periods in Altai. Problems of reconstruction of the climate and natural environment of the Holocene and Pleistocene of Siberia 2. Publishing House of the Institute of Archeology and Ethnog-

- raphy of the Siberian Branch of the Russian Academy of Sciences, Novosibirsk, 56–60. [In Russian]
- Bykov NI (2013) Vegetation of avalanche collections of Altai and the possibilities of phytoindication of avalanche processes. *Geography and nature management of Siberia* 15: 23–31. [In Russian]
- Bykov NI, Rygalova NV, Shigimaga AA (2024) Dendrochronological analysis of snow avalanches in the Northwestern Altai (Korgon river basin). *Ice and Snow* 64(1): 81–95. <https://doi.org/10.31857/S2076673424010066> [In Russian]
- Galakhov VP (2003) Conditions of formation and calculation of maximum snow reserves in the mountains (Based on the results of research in Altai). Publishing house «Nauka», Novosibirsk, 104 pp. [In Russian]
- Germain D, Héту B, Filion L (2010) Tree-Ring Based Reconstruction of Past Snow Avalanche Events and Risk Assessment in Northern Gaspé Peninsula (Québec, Canada). *Tree Rings and Natural Hazards: A State-of-the-Art, Advances in Global Change Research* 41: 51–73. [https://doi.org/10.1007/978-90-481-8736-2\\_5](https://doi.org/10.1007/978-90-481-8736-2_5)
- Germain D (2016) A statistical framework for tree-ring reconstruction of high-magnitude mass movements: case study of snow avalanches in Eastern Canada. *Geografiska Annaler: Series A, Physical Geography* 98(4): 303–311. <https://doi.org/10.1111/geoa.12138>
- Glaciological Dictionary (1984) Publishing house «Hydrometeoizdat», Leningrad, 526 pp. [In Russian]
- Kaennel M, Schweingruber FH (1995) Multilingual Glossary of Dendrochronology. Publishing House «Haupt», Bern, Stuttgart, Vienna, 467 pp.
- Koroleva TV (1993) Assessment of snowiness and avalanche danger of Altai on a medium scale. Abstract of a dissertation for the degree of Candidate of Geographical Sciences. Publishing House of Institute of Geography RAS, Moscow, 23 pp. [In Russian]
- Köse N, Aydın A, Yurtseven H, Akkemik Ü (2010) Using tree-ring signals and numerical model to identify the snow avalanche tracks in Kastamonu, Turkey. *Natural Hazards* 54(2): 435–449. <https://doi.org/10.1007/s11069-009-9477-x>
- Kravtsova VI (1971) Features of the regime of avalanche activity in the Altai according to dendrochronological observations. *Phytoindication methods in glaciology*. Publishing House of Moscow State University, Moscow, 103–123. [In Russian]
- Laute K, Beylich AA (2018) Potential effects of climate change on future snow avalanche activity in western Norway deduced from meteorological data. *Geografiska Annaler: Series A, Physical Geography* 100(2): 163–184. <https://doi.org/10.1080/04353676.2018.1425622>
- Martin J-P, Germain D (2016) Can we discriminate snow avalanches from other disturbances using the spatial patterns of tree-ring response? Case studies from the Presidential Range, White Mountains, New Hampshire, United States. *Dendrochronologia* 37: 17–32. <https://doi.org/10.1016/j.dendro.2015.12.004>

- Mundo IA, Barrera MD, Roig FA (2007) Testing the utility of *Nothofagus pumilio* for dating a snow avalanche in Tierra del Fuego, Argentina. *Dendrochronologia* 25(1): 19–28. <https://doi.org/10.1016/j.dendro.2007.01.001>
- Nikolaeva SA, Savchuk DA (2021) Evaluation of dendroindication methods for dating exogenous gravitational processes of the past in the upper reaches of the river. Aktru (Gorny Altai). Proceedings of the Russian Academy of Sciences. Geographic Series 85(3): 392–404. [In Russian]
- Perov VF, Turmanina VI, Akifeva KV (1977) Indications of avalanches and mud-flow by dendrochronology. Russian Papers on Dendrochronology and Dendroclimatology 1962, 1968, 1970, 1972. Research Laboratory for Archeology and history of Art. Oxford University, 49–51.
- Pop OT, Munteanu A, Flaviu M, Gavrilă I-G, Timofte C, Holobacă I-H (2017) Tree-ring-based reconstruction of high-magnitude snow avalanches in Piatra Craiului Mountains (Southern Carpathians, Romania). *Geografiska Annaler: Series A, Physical Geography* 100 (7):1–17. <https://doi.org/10.1080/04353676.2017.1405715>
- Revyakin VS, Kravtsova VI (1977) Snow cover and avalanches of Altai. Publishing house of Tomsk State University, Tomsk, 215 pp. [In Russian]
- Revyakin VS (1981) Natural ice of the Altai-Sayan mountain region. Publishing house «Gidrometeoizdat», Leningrad, 288 pp. [In Russian]
- Schweingruber FH (1993) Jahrringe und Umwelt – Dendroökologie. Eidgenössische Forschungsanstalt fuer Wald, Schnee und Landschaft, Birmensdorf, 474 pp.
- Speer JH (2010) Fundamentals of Tree-Ring Research. The University of Arizona Press, Tucson, 509 pp.
- Surnakov IV (1985) Some results of phytoindication of nival-glacial processes in Altai. Abstracts of the All-Union Conference “The role of nival-glacial formations in the dynamics of mountain ecosystems”. Publishing House of Altai State University, Barnaul, 35–36. [In Russian]
- Surnakov IV (1987) Some information about the elements of the nival-glacial complex of the upper reaches of the Bolshoy Abakan River. Abstracts of the reports of the scientific-practical conference “Glaciers and climate of Siberia”. Publishing House of Tomsk State University, Tomsk, 178–179. [In Russian]
- Turmanina VI (1979) Dendrochronology of avalanches in the upper reaches of the Baksan valley. Rhythms of glacial processes. Publishing House of Moscow State University, Moscow, 128–134. [In Russian]
- Tumajer J, Treml V (2015) Reconstruction ability of dendrochronology in dating avalanche events in the Giant Mountains, Czech Republic. *Dendrochronologia* 34: 1–9. <https://doi.org/10.1016/j.dendro.2015.02.002>
- Zubairov B, Lentschke J, Schröder H (2019) Dendroclimatology in Kazakhstan. *Dendrochronologia* 56: 125602. <https://doi.org/10.1016/j.dendro.2019.05.006>